Multivariable Nonlinear Control based on Exact Feedback Linearization with Integral Action for a PMSM

Sergio Velarde-Gomez, Eduardo Giraldo

***Abstract*—This paper introduces a novel approach for linear quadratic optimal control design for a nonlinear control structure based on a feedback linearization method and applied over permanent magnet synchronous motor (PMSM). The design of the proposed approach is developed by considering rotational speed, direct and quadrature currents as state variables. To achieve accurate tracking of the desired rotational speed, an additional nonlinear controller with integral action is implemented, also employing the exact feedback linearization method, and since the reference for the quadrature current is selected as zero only regulation is required. Consequently, a multivariable nonlinear controller is achieved using exact feedback linearization, offering robustness against external disturbances like torque load. The proposed method is assessed through simulations on a PMSM motor, and the speed reference tracking performance is analyzed with and without integral action. An additional comparison is carried out by incorporating a pole placement technique into the controller design. The proposed exact feedback linearization approach with integral action and linear quadratic control, demonstrates superior performance over other methods in terms of disturbance rejection, control effort and speed tracking.**

***Index Terms*—Nonlinear control, state space, exact feedback linearization, PMSM.**

I. Introduction

Permanent magnet synchronous motors (PMSMs) are favored over other motor types because of their high efficiency and power density [1] and simplified design [2], [3]. PMSMs can be classified between interior PMSM (I-PMSM) and surface-mounted PMSM (SM-PMSM) [4]. In [5] is shown that the SM-PMSM is commonly used for electric vehicle applications. The principal disadvantages of the PMSM are the demagnetization (exhibited in permanent magnets when faced with high temperature, [6]) and vibration environments, on top of its high cost [7]. Brushless DC motors based on permanent magnets (PM-BLDC) are known for their high efficiency, high power density, low electromagnetic interference, and reduced maintenance requirements. This motor is utilized in aerospace, servo applications, medical devices, robotics, and particularly in electric vehicles due to its excellent driving performance [8], [9], [10]. PMBLDC motors require electronic drivers because of their high torque and speed, and since they do not require brushes, a reduction in the copper and eddy current losses is obtained. In general, the use of permanent magnets eliminates excitation losses, thus increasing the motor's efficiency [10].

In [11] is presented a PMSM prototype constructed using additive manufacturing techniques, where several materials are considered. These PMSMs require a specifically designed structure for the magnets like the Halbach array. In [11] is also proposed an adaptive speed control of a 3D-printed permanent magnet synchronous motor (PMSM), which is designed and printed in PETG using a nine-pair pole structure with a Halbach array. The controller design validates the PMSM's performance even when constructed with non-ferromagnetic materials. In [12], an additional robust control design is performed for the PMSM described in [11], where the speed reference tracking is evaluated under noise conditions.

Several methods can be used for the control of nonlinear multivariable systems [13], such as state feedback linearization [14], gain scheduling, and sliding modes control [15]. For example, in [16] is proposed a buck converter control with integral action which is robust to disturbances but requires detailed knowledge of the system. In [17] is presented a multivariable sliding mode control of coupled tanks that show robustness to disturbances without a requirement of a detailed model of the system.

This study proposes an optimal linear quadratic design for a nonlinear controller based on the feedback linearization method in continuous time. The proposed approach is applied over a PMSM and evaluated for reference tracking. The zero steady state error is achieved by using integral action in the controller for non-zero references. A comparison analysis is performed by considering a pole placement technique, with and without integral action. The proposed approach is evaluated under external disturbances for rotational speed tracking and steady state error. This paper is organized as follows: in section II is presented the PMSM model in continuous time and the mathematical formulation of the integral multivariable nonlinear controller based on the exact feedback linearization approach. In section III are presented the results of the PMSM simulation and the reference tracking comparison under torque load disturbance, and finally, in section IV are presented the conclusions and future works.

II. Theoretical Framework

A. Continuous time Exact Feedback Linearization

The PMSM direct-quadrature framework model in continuous time can be described by the following

Manuscript received April 29, 2024; revised October 1, 2024.

Sergio Velarde-Gomez is a doctoral student in Electrical Engineering at Universidad Tecnológica de Pereira, Pereira, Colombia. Research Group in Automatic Control. E-mail: svelarde@utp.edu.co.

Eduardo Giraldo is a Full Professor at the Department of Electrical Engineering, Universidad Tecnológica de Pereira, Pereira, Colombia. Research group in Automatic Control. E-mail: egiraldos@utp.edu.co.

equations [18]:

$$\begin{aligned}\dot{x}_1 &= c_1x_1 + c_2x_2x_3 + c_3u_d\\ \dot{x}_2 &= c_4x_2 + c_5x_1x_3 + c_6x_3 + c_7u_q\\ \dot{x}_3 &= c_8x_2 + c_9x_1x_2 + c_{10}x_3 + c_{11}\tau_L\end{aligned} \tag{1}$$

where the state variables $x_1(t) = i_d(t)$, $x_2(t) = i_q(t)$ and $x_3(t) = \omega(t)$, and where the PMSM outputs are defined by

$$\begin{aligned}y_1 &= h_1(x) = x_1\\ y_2 &= h_2(x) = x_3\end{aligned} \tag{2}$$

The exact feedback linearization approach requires the apllication of successive derivatives of the outputs until an input appears [13]. Assuming the model (1) with $T_L(t) = 0$, for the first output, it follows:

$$\dot{y}_1 = \frac{dh_1}{dt} \tag{3}$$
$$\dot{y}_1 = \dot{x}_1 = c_1x_1 + c_2x_2x_3 + c_3u_d \tag{4}$$
$$\dot{y}_1 = L_fh_1(x) + L_{g_d}h_1(x)u_d \tag{5}$$

being

$$L_fh_1(x) = c_1x_1 + c_2x_2x_3 \tag{6}$$
$$L_{g_d}h_1(x) = c_3 \tag{7}$$

since the input $u_d(t)$ appears, the derivatives of this input are stopped, and the control signal $v_1(t)$ is computed as:

$$\dot{y}_1 = v_1 \tag{8}$$

For the second output, it follows:

$$\dot{y}_2 = \frac{dh_2}{dt} \tag{9}$$
$$\dot{y}_2 = \dot{x}_3 = c_8x_2 + c_9x_1x_2 + c_{10}x_3 \tag{10}$$
$$\dot{y}_2 = L_fh_2(x) + L_{g_d}h_2(x)u_d + L_{g_q}h_2(x)u_q \tag{11}$$

being

$$L_fh_2(x) = c_8x_2 + c_9x_1x_2 + c_{10}x_3 \tag{12}$$
$$L_{g_d}h_2(x) = 0 \tag{13}$$
$$L_{g_q}h_2(x) = 0 \tag{14}$$

Then, the successive derivative is obtained as

$$\ddot{y}_2 = \frac{d^2h_2}{dt^2} \tag{15}$$
$$\ddot{y}_2 = c_9x_2\dot{x}_1 + (c_8 + c_9x_1)\dot{x}_2 + c_{10}\dot{x}_3 \tag{16}$$
$$\begin{aligned}\ddot{y}_2 &= c_9x_2(c_1x_1 + c_2x_2x_3 + c_3u_d)\\ &+ (c_8 + c_9x_1)(c_4x_2 + c_5x_1x_3 + c_6x_3 + c_7u_q)\\ &+ c_{10}(c_8x_2 + c_9x_1x_2 + c_{10}x_3)\end{aligned} \tag{17}$$

It follows that

$$\begin{aligned}\ddot{y}_2 &= c_1c_9x_1x_2 + c_2c_9x_2^2x_3 + c_3c_9x_2u_d + c_4c_8x_2\\ &+ c_5c_8x_1x_3 + c_6c_8x_3 + c_7c_8u_q\\ &+ c_4c_9x_1x_2 + c_5c_9x_1^2x_3 + c_6c_9x_3 + c_7c_9x_1u_q\\ &+ c_8c_{10}x_2 + c_9c_{10}x_1x_2 + c_{10}^2x_3\end{aligned} \tag{18}$$
$$\ddot{y}_2 = L_f^2h_2(x) + L_{g_d}L_fh_2(x)u_d + L_{g_q}L_fh_2(x)u_q \tag{19}$$

being

$$\begin{aligned}L_f^2h_2(x) &= c_1c_9x_1x_2 + c_2c_9x_2^2x_3 + c_4c_8x_2\\ &+ c_5c_8x_1x_3 + c_6c_8x_3 + c_4c_9x_1x_2\\ &+ c_5c_9x_1^2x_3 + c_6c_9x_3 + c_8c_{10}x_2\\ &+ c_9c_{10}x_1x_2 + c_{10}^2x_3\end{aligned} \tag{20}$$
$$L_{g_d}L_fh_2(x) = c_3c_9x_2 \tag{21}$$
$$L_{g_q}L_fh_2(x) = c_7c_8 + c_7c_9x_1 \tag{22}$$

and since the inputs $u_d(t)$ and $u_q(t)$ appear, the derivatives of this output are stopped. Therefore, the control signal $v_2(t)$ is defined as

$$\ddot{y}_2 = v_2 \tag{23}$$

The resulting system is

$$\begin{bmatrix}\dot{y}_1\\ \dot{y}_2\\ \ddot{y}_2\end{bmatrix} = \underbrace{\begin{bmatrix}0 & 0 & 0\\ 0 & 0 & 1\\ 0 & 0 & 0\end{bmatrix}}_{A}\begin{bmatrix}y_1\\ y_2\\ \dot{y}_2\end{bmatrix} + \underbrace{\begin{bmatrix}1 & 0\\ 0 & 0\\ 0 & 1\end{bmatrix}}_{B}\begin{bmatrix}v_1\\ v_2\end{bmatrix} \tag{24}$$

$$\begin{bmatrix}y_1\\ y_2\end{bmatrix} = \underbrace{\begin{bmatrix}1 & 0 & 0\\ 0 & 1 & 0\end{bmatrix}}_{C}\begin{bmatrix}y_1\\ y_2\\ \dot{y}_2\end{bmatrix} \tag{25}$$

Considering the structure of (24) it can be written as two subsystems. For the first subsystem, it follows that

$$[\dot{y}_1] = \underbrace{[0]}_{a_1}[y_1] + \underbrace{[1]}_{b_1}[v_1] \tag{26}$$
$$[y_1] = \underbrace{[1]}_{c_1}[y_1] \tag{27}$$

where $v_1(t)$ is defined by

$$v_1 = -k_1y_1 \tag{28}$$
$$v_1 = -k_1x_1 \tag{29}$$

After designed, and by considering that

$$v_1 = L_fh_1(x) + L_{g_d}h_1(x)u_d \tag{30}$$
$$v_1 = -k_1x_1 \tag{31}$$

the control law for $u_d(t)$ can be obtained, as follows:

$$u_d = \frac{1}{L_{g_d}h_1(x)}(-k_1x_1 - L_fh_1(x)) \tag{32}$$
$$u_d = \frac{1}{c_3}(-k_1x_1 - c_1x_1 - c_2x_2x_3) \tag{33}$$

In a similar way, for the second subsystem it follows that

$$\begin{bmatrix}\dot{y}_2\\ \ddot{y}_2\end{bmatrix} = \underbrace{\begin{bmatrix}0 & 1\\ 0 & 0\end{bmatrix}}_{A_2}\begin{bmatrix}y_2\\ \dot{y}_2\end{bmatrix} + \underbrace{\begin{bmatrix}0\\ 1\end{bmatrix}}_{B_2}[v_2] \tag{34}$$

$$[y_2] = \underbrace{[1 \quad 0]}_{C_2}\begin{bmatrix}y_2\\ \dot{y}_2\end{bmatrix} \tag{35}$$

where the control law for $v_2(t)$, considering integral action, is defined by

$$v_2 = -k_2y_2 - k_3\dot{y}_2 + k_ie_i \tag{36}$$
$$v_2 = -k_2x_3 - k_3\dot{x}_3 + k_ie_i \tag{37}$$
$$v_2 = -k_2x_3 - k_3(c_8x_2 + c_9x_1x_2 + c_{10}x_3) + k_ie_i \tag{38}$$

being e_i the error integral, defined as

$$e_i = \int_0^t (\omega_{ref}(\tau) - x_3(\tau))d\tau \tag{39}$$

being ω_{ref} the reference for ω. Therefore, e_i can be also defined as follows

$$\dot{e_i} = \omega_{ref} - x_3 \tag{40}$$

By considering (40), an augmented state space system can be obtained as follows

$$\begin{bmatrix} \dot{y}_2 \\ \ddot{y}_2 \\ \dot{e}_i \end{bmatrix} = \underbrace{\begin{bmatrix} 0 & 1 & 0 \\ 0 & 0 & 0 \\ -1 & 0 & 0 \end{bmatrix}}_{A_a} \begin{bmatrix} y_2 \\ \dot{y}_2 \\ e_i \end{bmatrix} + \underbrace{\begin{bmatrix} 0 \\ 1 \\ 0 \end{bmatrix}}_{B_a} \begin{bmatrix} v_2 \end{bmatrix} + \underbrace{\begin{bmatrix} 0 \\ 0 \\ 1 \end{bmatrix}}_{B_r} \begin{bmatrix} \omega_{ref} \end{bmatrix} \tag{41}$$

with v_2 defined as

$$v_2 = \underbrace{\begin{bmatrix} k_2 & k_3 & -k_i \end{bmatrix}}_{K_a} \begin{bmatrix} y_2 \\ \dot{y}_2 \\ e_i \end{bmatrix} \tag{42}$$

After designed, and by considering that

$$v_2 = L_f^2 h_2(x) + L_{g_d} L_f h_2(x) u_d \tag{43}$$
$$+ L_{g_q} L_f h_2(x) u_q \tag{44}$$
$$v_2 = -k_2 x_3 - k_3 \dot{x}_3 + k_i e_i \tag{45}$$

the control law for $u_q(t)$ can be obtained, as follows:

$$u_q = \frac{1}{L_{g_q} L_f h_2(x)} \left(k_i e_i - k_2 x_3 - k_3 \dot{x}_3 - L_f^2 h_2(x) - L_{g_d} L_f h_2(x) u_d \right) \tag{46}$$

$$\begin{aligned} u_q = \frac{1}{c_7 c_8 + c_7 c_9 x_1} (& k_i e_i - k_2 x_3 \\ & - k_3 (c_8 x_2 + c_9 x_1 x_2 + c_{10} x_3) \\ & - (c_1 c_9 x_1 x_2 + c_2 c_9 x_2^2 x_3 \\ & + c_4 c_8 x_2 + c_5 c_8 x_1 x_3 + c_6 c_8 x_3 \\ & + c_4 c_9 x_1 x_2 + c_5 c_9 x_1^2 x_3 + c_6 c_9 x_1 x_3 \\ & + c_8 c_{10} x_2 + c_9 c_{10} x_1 x_2 + c_{10}^2 x_3) \\ & - c_9 x_2 (-k_1 x_1 - c_1 x_1 - c_2 x_2 x_3)) \end{aligned} \tag{47}$$

$$\begin{aligned} u_q = \frac{1}{c_7 c_8 + c_7 c_9 x_1} (& k_i e_i - k_2 x_3 \\ & - k_3 (c_8 x_2 + c_9 x_1 x_2 + c_{10} x_3) \\ & - (c_4 c_8 x_2 + c_5 c_8 x_1 x_3 + c_6 c_8 x_3 \\ & + c_4 c_9 x_1 x_2 + c_5 c_9 x_1^2 x_3 + c_6 c_9 x_1 x_3 \\ & + c_8 c_{10} x_2 + c_9 c_{10} x_1 x_2 + c_{10}^2 x_3) + c_9 x_1 x_2 k_1) \end{aligned} \tag{48}$$

By assuming the parameter $c_9 = 0$, and the control equation for u_q can be reduced as follows:

$$\begin{aligned} u_q = \frac{1}{c_7 c_8} (& k_i e_i - k_2 x_3 - k_3 (c_8 x_2 + c_{10} x_3) \\ & - (c_4 c_8 x_2 + c_5 c_8 x_1 x_3 + c_6 c_8 x_3 + c_8 c_{10} x_2 + c_{10}^2 x_3)) \end{aligned} \tag{49}$$

In Fig. 1 is shown an schematic diagram of the PMSM exact feedback nonlinear control with integral action.

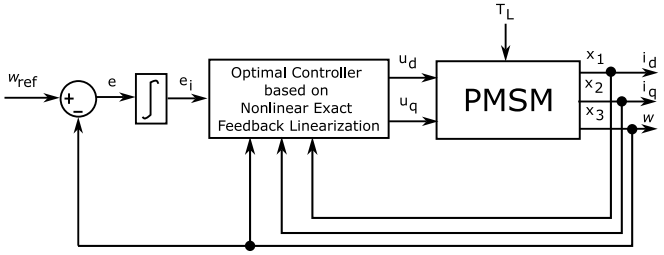

Fig. 1. Schematic diagram of the PMSM exact feedback nonlinear control with integral action

B. Controller gains design

A Linear Quadratic Regulator (LQR) controller can be designed based on the state feedback structure. For control law v_1, it follows that

$$J_1 = \int_0^t (q_1 x_1^2(\tau) + r_1 v_1^2(\tau))d\tau \tag{50}$$

where q_1 and r_1 are the weights related to x_1 and v_1 respectively. For control law v_2, it follows that

$$J_2 = \int_0^t (x_a^T(\tau) Q_a x_a(\tau) + r_2 v_2^2(\tau))d\tau \tag{51}$$

being the augmented states x_a defined as

$$x_a = \begin{bmatrix} y_2 \\ \dot{y}_2 \\ e_i \end{bmatrix} \tag{52}$$

and the Q_a and r_2, the weights related to x_a and v_2 respectively. Where Q_a is defined as

$$Q_a = \begin{bmatrix} q_2 & 0 & 0 \\ 0 & q_3 & 0 \\ 0 & 0 & q_i \end{bmatrix} \tag{53}$$

being q_2 the weight related to y_2, q_3 the weight related to $\dot{y}_2$, and q_i the weight related to e_i.

III. Results

The proposed control approach is evaluated over a PMSM Teknic-2310P with the following set of c_j parameters

$$\begin{aligned} c_1 = -1.8 \times 10^3, c_2 = 4, c_3 = 5000 \\ c_4 = -1.8 \times 10^3, c_5 = -4, c_6 = -127.9083 \\ c_7 = 5000, c_8 = 5.434 \times 10^3, c_9 = 0 \\ c_{10} = -0.3734, c_{11} = -1.4165 \times 10^5 \end{aligned}$$

By considering these parameters, the following continuous time model is obtained

$$\begin{aligned} \dot{x}_1 &= -1.8 \times 10^3 x_1 + 4 x_2 x_3 + 5000 u_d \\ \dot{x}_2 &= -1.8 \times 10^3 x_2 - 4 x_1 x_3 \\ &\quad - 127.9083 x_3 + 5000 u_q \\ \dot{x}_3 &= 5.434 \times 10^3 x_2 - 0.3734 x_3 \\ &\quad - 1.4165 \times 10^5 \tau_L \end{aligned} \tag{54}$$

and also, the following control law is obtained for u_d

$$u_d = \frac{1}{c_3} (-k_1 x_1 - c_1 x_1 - c_2 x_2 x_3)$$
$$u_d = \frac{1}{5000} \left(-k_1 x_1 + 1.8 \times 10^3 x_1 - 4 x_2 x_3 \right)$$

and u_q

$$
\begin{aligned}
u_q = & \frac{1}{c_7 c_8}\left(k_i e_i - k_2 x_3 - k_3(c_8 x_2 + c_{10} x_3)\right. \\
& - c_4 c_8 x_2 - c_5 c_8 x_1 x_3 - c_6 c_8 x_3 \\
& \left. - c_8 c_{10} x_2 - c_{10}^2 x_3\right) \\
u_q = & \frac{1}{2.7170 \times 10^7}\left(k_i e_i - k_2 x_3\right. \\
& - k_3(5.434 \times 10^3 x_2 - 0.3734 x_3) \\
& + 9.7811 \times 10^6 x_2 + 2.1736 \times 10^4 x_1 x_3 \\
& + 6.9505 \times 10^5 x_3 \\
& \left. + 2.0291 \times 10^3 x_2 - 0.1394 x_3\right)
\end{aligned}
$$

The open-loop system response by considering step inputs for u_d, u_q and τ_L shown in Fig. 2 is shown in Fig. 3

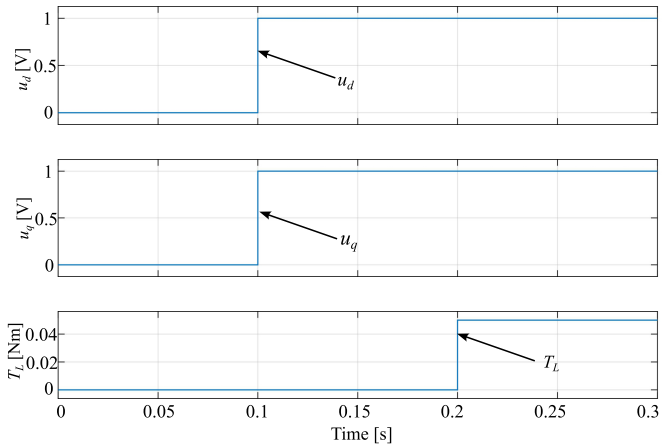

Fig. 2. Open loop inputs

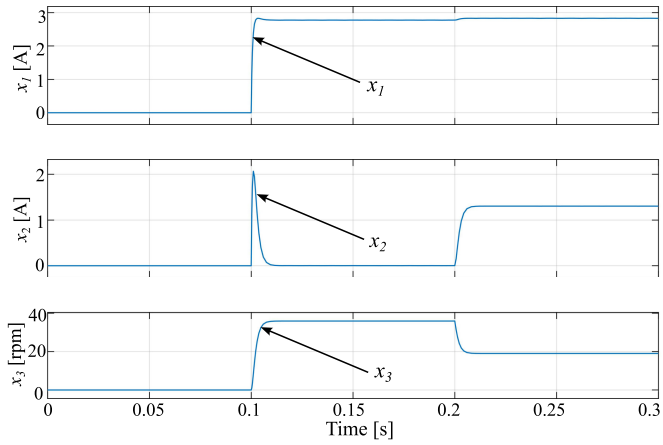

Fig. 3. Open loop outputs

The block diagram that represents the PMSM system in continuous time is shown in Fig. 4

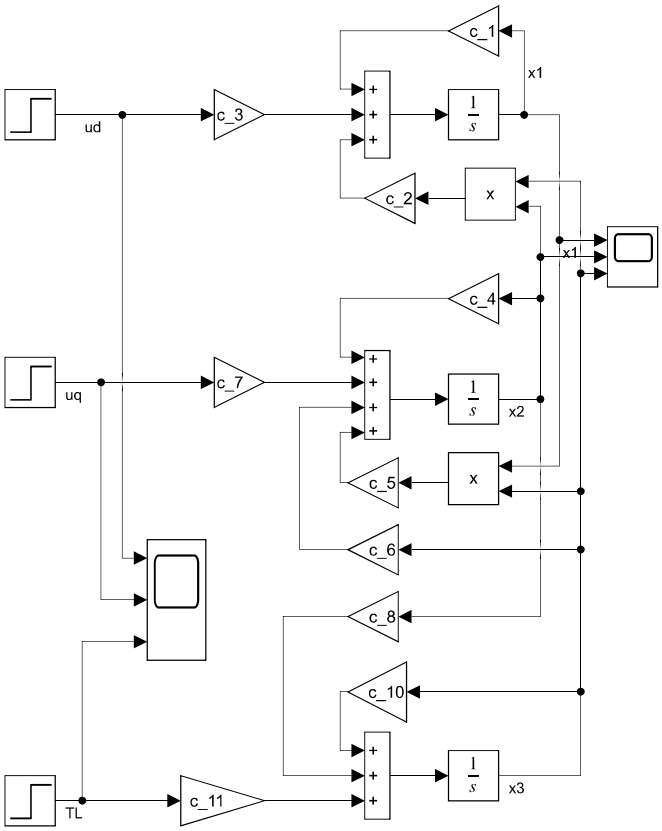

Fig. 4. Nonlinear multivariable model of the PMSM in continuous time

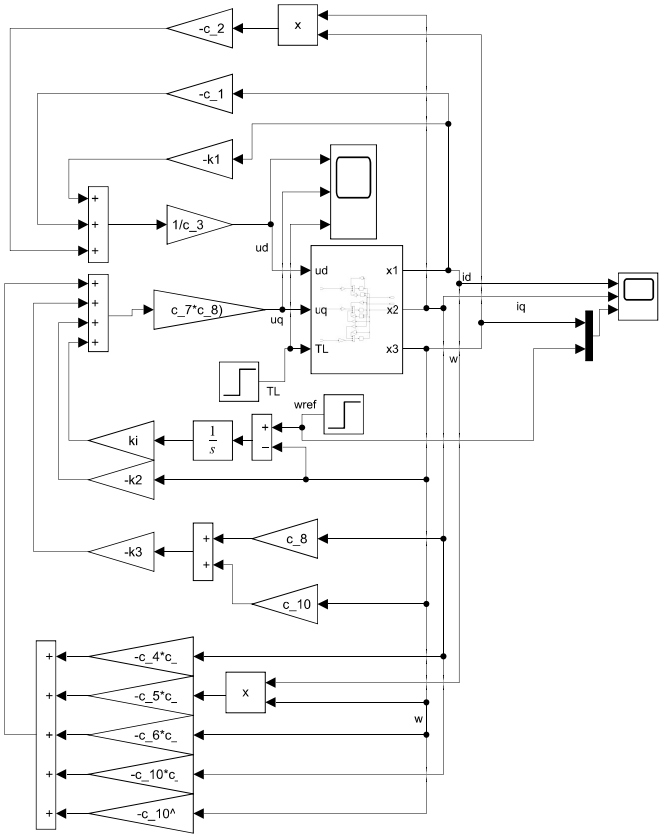

Fig. 5. Nonlinear control based on exact feedback linearization with integral action in continuous time

In order to evaluate the performance of the proposed exact feedback linearization approach with the optimal control

design, a comparison analysis is performed by using a pole placement based control design with two controller configuration: with and without integral action.

The block diagram that represents the exact feedback nonlinear control of the PMSM system with integral action is shown in Fig. 5.

The design of the controller gains by using a LQR controller can be performed by selecting the weights as follows

$$q_1 = 1000000 \tag{55}$$
$$r_1 = 1 \tag{56}$$
$$Q_a = \begin{bmatrix} 0 & 0 & 0 \\ 0 & 0 & 0 \\ 0 & 0 & 5000000000 \end{bmatrix} \tag{57}$$
$$r_2 = 1 \tag{58}$$

which results in the following controller gains

$$k_1 = 1000 \tag{59}$$
$$k_2 = 3420 \tag{60}$$
$$k_3 = 82.7037 \tag{61}$$
$$k_i = 70711 \tag{62}$$

The closed-loop response by using the exact feedback nonlinear control technique and the optimal control and by considering the inputs for u_d, u_q and τ_L shown in Fig. 6 is shown in Fig. 7

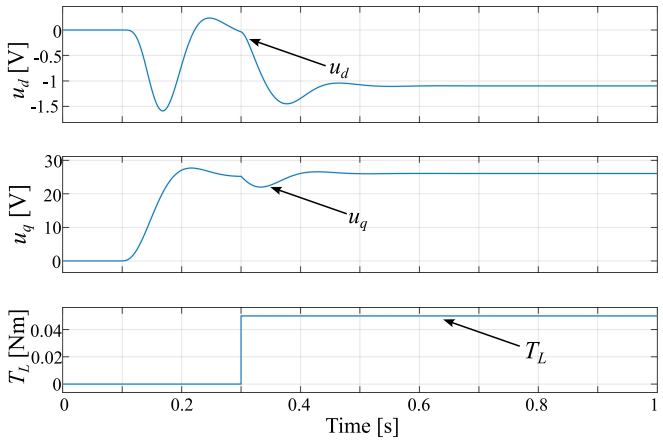

Fig. 6. Closed loop inputs of the nonlinear control based on exact feedback linearization with integral action and optimal control

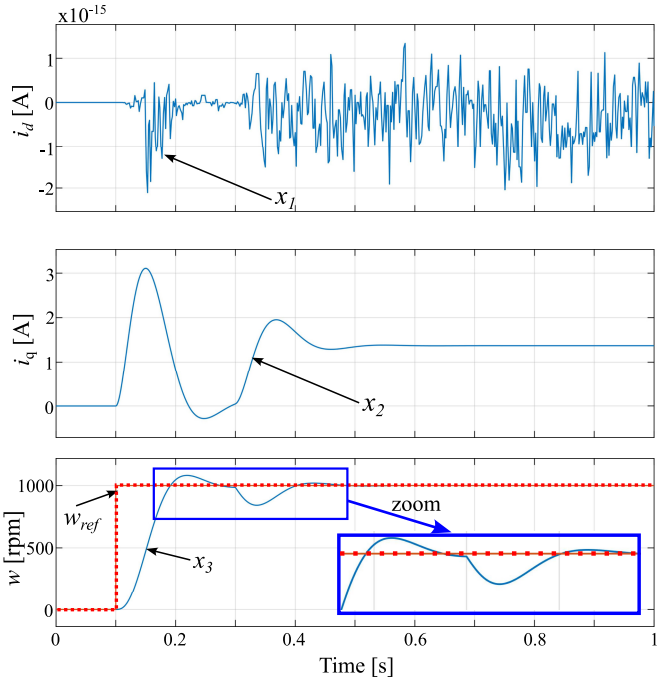

Fig. 7. Closed loop outputs of the nonlinear control based on exact feedback linearization with integral action and optimal control

If the exact feedback controller is designed without considering the integral action, it follows that the control signal u_q is therefore computed as

$$\begin{aligned} u_q = & \frac{1}{c_7 c_8}\left(k_2(w_{ref} - x_3) - k_3(c_8 x_2 + c_{10} x_3)\right. \\ & - c_4 c_8 x_2 - c_5 c_8 x_1 x_3 - c_6 c_8 x_3 \\ & \left. -c_8 c_{10} x_2 - c_{10}^2 x_3\right) \\ u_q = & \frac{1}{2.7170 \times 10^7}\left(k_2(w_{ref} - x_3)\right. \\ & - k_3(5.434 \times 10^3 x_2 - 0.3734 x_3) \\ & + 9.7811 \times 10^6 x_2 + 2.1736 \times 10^4 x_1 x_3 + 6.9505 \times 10^5 x_3 \\ & \left. +2.0291 \times 10^3 x_2 - 0.1394 x_3\right) \end{aligned}$$

In Fig. 8 is shown the schematic diagram of the PMSM nonlinear control based on exact feedback linearizarion without integral action.

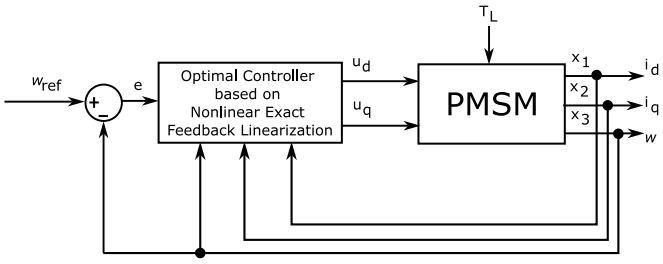

Fig. 8. Schematic diagram of the PMSM nonlinear control based on exact feedback linearizarion without integral action

The block diagram that represents the exact feedback nonlinear control of the PMSM system without integral action is shown in Fig. 9.

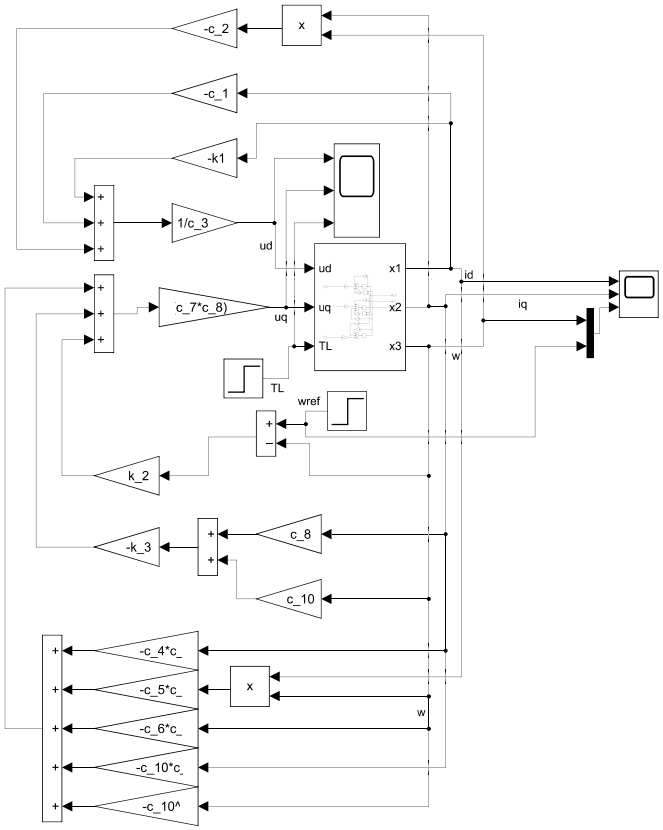

Fig. 9. Nonlinear control based on exact feedback linearization without integral action

The design of the controller gains by using a LQR controller without integral action can be performed by selecting the weights as follows

$$q_1 = 1000000 \tag{63}$$
$$r_1 = 1 \tag{64}$$
$$Q = \begin{bmatrix} 5000000 & 0 \\ 0 & 0 \end{bmatrix} \tag{65}$$
$$r_2 = 1 \tag{66}$$

which results in the following controller gains

$$k_1 = 1000 \tag{67}$$
$$k_2 = 2236.1 \tag{68}$$
$$k_3 = 66.87 \tag{69}$$

The closed-loop response by using the exact feedback nonlinear control technique and the optimal control without integral action and by considering the inputs for u_d, u_q and τ_L shown in Fig. 10 is shown in Fig. 11

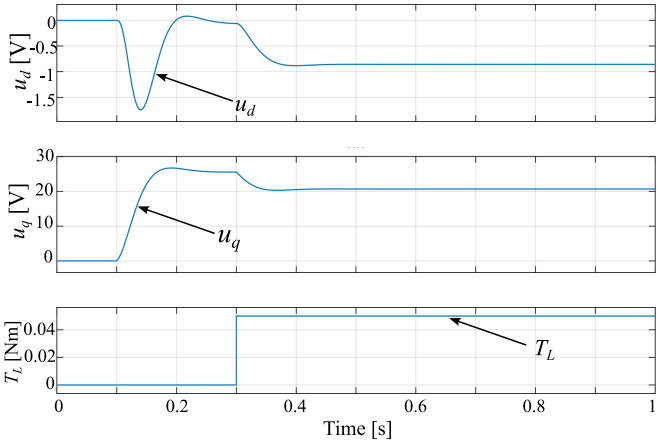

Fig. 10. Closed loop inputs of the nonlinear control based on exact feedback linearization without integral action and optimal control

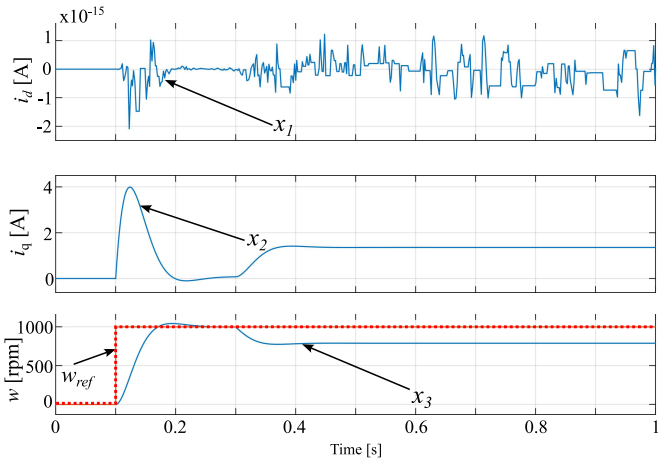

Fig. 11. Closed loop outputs of the nonlinear control based on exact feedback linearization without integral action and optimal control

For the sake of comparison, the design of the controller gains k_1, k_2, k_3 and k_i are also designed by considering a pole placement technique with settling time t_s of 100 milliseconds, as follows:

$$t_s = \frac{4}{p} \tag{70}$$
$$p = \frac{4}{0.1} = 40 \tag{71}$$

being p the magnitude of the dominant pole.

Therefore, for the controller gain k_1 it follows that

$$p_1(s) = s + k1 = s + 40 \tag{72}$$

and therefore

$$k1 = 40 \tag{73}$$

and for the controller gains k_2, k_3, and k_i it follows that

$$p_2(s) = \det \begin{pmatrix} s & -1 & 0 \\ k_2 & s + k_3 & -k_i \\ 1 & 0 & s \end{pmatrix} \tag{74}$$
$$p_2(s) = s^3 + k_3 s^2 + k_2 s + k_i \tag{75}$$
$$p_2(s) = (s + 40)(s + 160)^2 \tag{76}$$

resulting in

$$k_2 = 38400 \tag{77}$$
$$k_3 = 360 \tag{78}$$
$$k_i = 1024000 \tag{79}$$

By considering these parameters, the closed-loop response by using the exact feedback nonlinear control with integral action and the pole placement technique, and by considering the inputs for u_d, u_q and τ_L shown in Fig. 12 is shown in Fig. 13

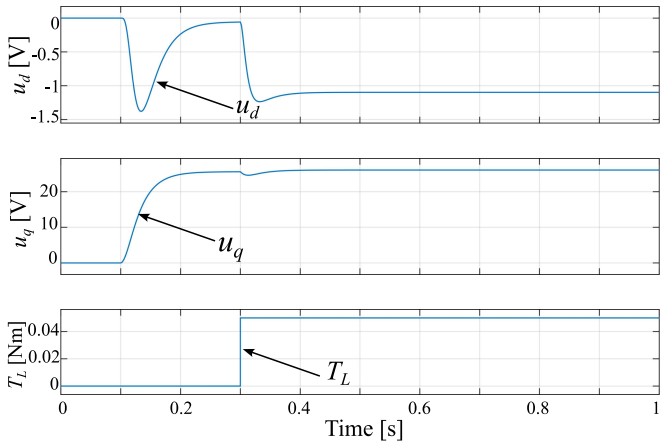

Fig. 12. Closed loop inputs of the nonlinear control based on exact feedback linearization with integral action and pole placement technique

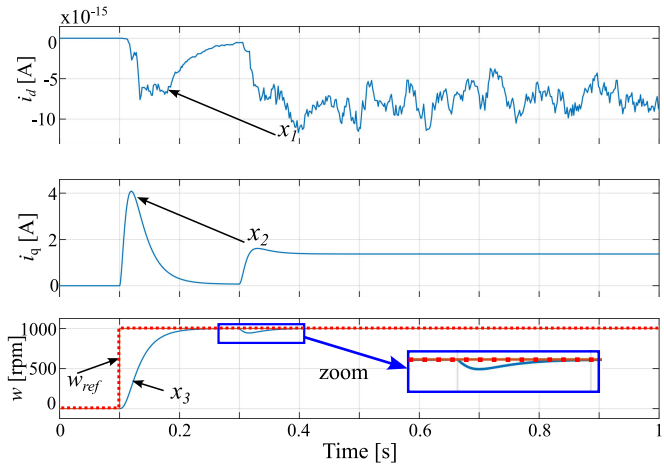

Fig. 13. Closed loop outputs of the nonlinear control based on exact feedback linearization with integral action and pole placement technique

In addition, if the exact feedback controller is designed without the integral action by the pole placement technique, the controller gains k_2 and k_3 can be designed as follows

$$p_2(s) = \det \begin{pmatrix} s & -1 \\ k_2 & s + k_3 \end{pmatrix} \tag{80}$$
$$p_2(s) = s^2 + k_3 s + k_2 \tag{81}$$
$$p_2(s) = (s + 40)(s + 160) \tag{82}$$

resulting in

$$k_2 = 6400 \tag{83}$$
$$k_3 = 200 \tag{84}$$

By considering these parameters, the closed-loop response by using the exact feedback nonlinear control without integral action and the pole placement technique, and by considering the inputs for u_d, u_q and τ_L shown in Fig. 14 is shown in Fig. 15

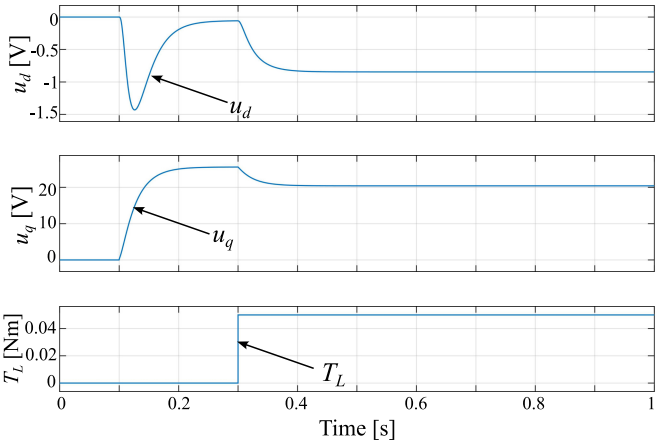

Fig. 14. Closed loop inputs of the nonlinear control based on exact feedback linearization without integral action and pole placement technique

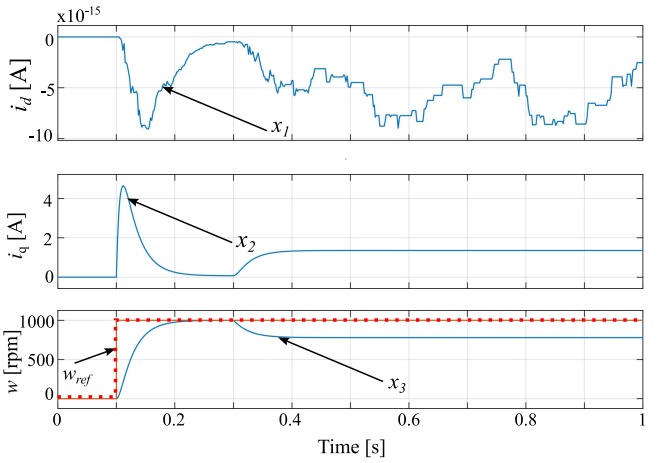

Fig. 15. Closed loop outputs of the nonlinear control based on exact feedback linearization without integral action and pole placement technique

In Table I is shown a comparison in terms of the stationary error of the proposed exact feedback controller (EFC) approach with and without optimal computation of the controller gains by using the optimal control approach and the pole-placement approach.

TABLE I
STATIONARY ERROR COMPARISON OF THE PROPOSED EFC APPROACH BY CONSIDERING OPTIMAL AND POLE-PLACEMENT GAINS

Controller Gains	EFC with Integral Action	EFC without Integral Action
Optimal	0.01 rpm	170.5 rpm
Pole-placement	0.01 rpm	180.2 rpm

It is worth noting that in Table I, it is shown that the stationary error for speed tracking is near zero for the proposed EFC approach by considering integral action even when the controller gains are computed by using an optimal approach or a pole-placement approach. On the other hand, the EFC approach without the integral action shows a

stationary error near 180 rpm for controller gains computed by an optimal approach or a pole-placement approach.

IV. Conclusions

In this work is presented an optimal control design based on a linear quadratic regulator to obtain a nonlinear multivariable controller based on the exact feedback linearization technique with integral action. By considering the mathematical formulation proposed in section II, the design of the nonlinear multivariable controller is reduced to two linearized independent state space subsystems, and it is straightforwardly converted to a nonlinear state feedback controller by using the exact feedback linearization approach. As a result it can be seen that the control effort of signals u_d and u_q require less amplitude by using the optimal control design than with the pole placement design, reducing the magnitudes of the i_d and i_q currents. In addition, it can be seen that the proposed approach by considering integral action shows a stationary error near to zero even when the controller gains are computed by an optimal or a pole-placement approach. For future work, it can be considered that since the proposed approach is evaluated by using real PMSM motor parameters, the proposed approach can be directly validated in a real environment.

References

[1] W. Xu, M. M. Ismail, Y. Liu, and M. R. Islam, "Parameter optimization of adaptive flux-weakening strategy for permanent-magnet synchronous motor drives based on particle swarm algorithm," *IEEE Transactions on Power Electronics*, vol. 34, no. 12, pp. 12 128–12 140, 2019.

[2] C. Gong, Y. Hu, J. Gao, Y. Wang, and L. Yan, "An improved delay-suppressed sliding-mode observer for sensorless vector-controlled pmsm," *IEEE Transactions on Industrial Electronics*, vol. 67, no. 7, pp. 5913–5923, 2020.

[3] P. Gao, G. Zhang, H. Ouyang, and L. Mei, "A sliding mode control with nonlinear fractional order pid sliding surface for the speed operation of surface-mounted pmsm drives based on an extended state observer," *Mathematical Problems in Engineering*, vol. 2019, no. 1, p. 7130232, 2019. [Online]. Available: https://onlinelibrary.wiley.com/doi/abs/10.1155/2019/7130232

[4] X. Sun, Z. Li, X. Wang, and C. Li, "Technology development of electric vehicles: A review," *Energies*, vol. 13, no. 1, 2020. [Online]. Available: https://www.mdpi.com/1996-1073/13/1/90

[5] C. Gong, Y. Hu, K. Ni, J. Liu, and J. Gao, "Sm load torque observer-based fcs-mpdsc with single prediction horizon for high dynamics of surface-mounted pmsm," *IEEE Transactions on Power Electronics*, vol. 35, no. 1, pp. 20–24, 2020.

[6] K. Zhao, N. Jia, J. She, W. Dai, R. Zhou, W. Liu, and X. Li, "Robust model-free super-twisting sliding-mode control method based on extended sliding-mode disturbance observer for pmsm drive system," *Control Engineering Practice*, vol. 139, p. 105657, 2023. [Online]. Available: https://www.sciencedirect.com/science/article/pii/S0967066123002265

[7] S. Xiao and A. Griffo, "Pwm-based flux linkage and rotor temperature estimations for permanent magnet synchronous machines," *IEEE Transactions on Power Electronics*, vol. 35, no. 6, pp. 6061–6069, 2020.

[8] P. Kumar, D. V. Bhaskar, U. R. Muduli, A. R. Beig, and R. K. Behera, "Iron-loss modeling with sensorless predictive control of pmbldc motor drive for electric vehicle application," *IEEE Transactions on Transportation Electrification*, vol. 7, no. 3, pp. 1506–1515, 2021.

[9] K. Karthick, S. Ravivarman, R. Samikannu, K. Vinoth, and B. Sasikumar, "Analysis of the impact of magnetic materials on cogging torque in brushless dc motor," *Advances in Materials Science and Engineering*, vol. 2021, no. 1, p. 5954967, 2021. [Online]. Available: https://onlinelibrary.wiley.com/doi/abs/10.1155/2021/5954967

[10] A. Darcy, G. Jegha, P. Subathra, N. Manoj Kumar, U. Subramaniam, and S. Padmanaban, "A High Gain DC-DC Converter with Grey Wolf Optimizer Based MPPT Algorithm for PV Fed BLDC Motor Drive," *Applied Sciences*, vol. 10, p. 2797, 2020. [Online]. Available: https://www.mdpi.com/2076-3417/10/8/2797

[11] S. Velarde-Gomez, A. Molina-Cabrera, and E. Giraldo, "Model-based adaptive control of a 3d printed permanent magnet synchronous motor," *Engineering Letters*, vol. 31, no. 4, pp. 1804–1812, 2023.

[12] S. Velarde-Gomez and E. Giraldo, "Robust state space embedded control of a 3d printed permanent magnet synchronous motor," *IAENG International Journal of Applied Mathematics*, vol. 54, no. 2, pp. 255–261, 2024.

[13] S. Sastry, *Nonlinear Systems: Analysis, Stability, and Control*, ser. Interdisciplinary Applied Mathematics. Springer New York, 2013.

[14] S. Velarde-Gomez and E. Giraldo, "Real-time identification and nonlinear control of a permanent-magnet synchronous motor based on a physics-informed neural network and exact feedback linearization," *Information*, vol. 15, no. 9:577, pp. 1–23, 2024.

[15] H. Sira-Ramirez, R. Marquez, F. Rivas-Echeverria, and O. Llanea-Santiago, *Control de sistemas no lineales: Linealizacion aproximada, extendida y exacta*. New York: Pearson - Prentice Hall, 2005.

[16] J. S. Velez-Ramirez, L. A. Rios-Norena, and E. Giraldo, "Buck converter current and voltage control by exact feedback linearization with integral action," *Engineering Letters*, vol. 29, no. 1, pp. 168–176, 2021.

[17] F. Osorio-Arteaga, D. Giraldo-Buitrago, and E. Giraldo, "Sliding mode control applied to mimo systems," *Engineering Letters*, vol. 27, no. 4, pp. 802–806, 2019.

[18] M. Nicola and C.-I. Nicola, "Improvement of linear and nonlinear control for pmsm using computational intelligence and reinforcement learning," *Mathematics*, vol. 10, no. 24, 2022. [Online]. Available: https://www.mdpi.com/2227-7390/10/24/4667